



Transient Performance Improvement of Thermal System Connected to Grid Using Distributed Generation and Capacitive Energy Storage Unit

A. Chatterjee¹, S. P. Ghoshal², and V. Mukherjee³

¹Department of Electrical Engineering, Asansol Engineering College, Asansol, West Bengal, India

²Department of Electrical Engineering, National Institute of Technology, Durgapur, West Bengal, India

³Department of Electrical Engineering, Indian School of Mines, Dhanbad, Jharkhand, India

vivek_agamani@yahoo.com

Abstract: In this paper, a conventional thermal power plant with single stage reheat turbine is taken into consideration. It is equipped with AVR, IEEE type dual input PSS3B and integral controlled AGC loop. A hybrid distributed generation (DG) system consisting of wind turbine generators, aqua electrolyzer, fuel cells, diesel engine generator, flywheel energy storage system and battery energy storage system is configured. This hybrid DG system is integrated with the grid connected thermal unit. The different tunable parameters of this integrated power system are optimized by a novel craziness-based PSO with wavelet mutation (CRPSOWM), developed by the authors. While integrating the DG with the thermal power system, improved transient performance is noticed. Further improvement in the transient performance is observed with the usage of capacitive energy storage unit in the AGC loop of conventional power generation scheme. The proposed CRPSOWM incorporates a wavelet-theory-based mutation operation and offers robust and promising results.

Keywords: Aqua electrolyzer; capacitive energy storage; craziness-based particle swarm optimization with wavelet mutation; diesel engine generator; energy storage devices; fuel cell; wavelet mutation; wind turbine generator

1. Introduction

In the recent years, power sectors are meeting difficulties arisen out of anticipated load demand of the consumers. Petroleum price hike is worsening the energy crisis more. More efficient and reliable operation of the power industries is, therefore, the real call of the day. Increased emphasis is being paid by the researchers and practicing engineers for improved performance of the existing system.

Various distributed generations (DGs) are coming into operation to fulfill the load demand. With the deregulation of power sector, independent power producers (IPPs) are participating in the power market. IPPs are supplying reliable power to the consumers [1-2]. In addition, it also allows businesses to save on electricity costs by using their units during high peak demand periods when power is most expensive. DGs not only offer reliable, economical and efficient operation of power sector, but these also offer less environmental pollution and reduce green house effect [3-4]. For example, hydrogen fuel cell is an environmental friendly generating system used in DGs.

Renewable sources of energy are under the umbrella of DG. Several types of small scale generation systems can be used for DG. These may include wind turbine generator (WTG), aqua electrolyzer (AE), fuel cell (FC), diesel engine generator (DEG) etc. Cost of electricity generation from wind energy has come down and may be as close to as traditional fossil fuel energies. Wind energy is considered as one of the most rapidly growing energy resources all over the world. It is expected that about 12% of the total world electricity demands will be supplied from wind energy resources by 2020[5]. Wind is an innovative, clean, and intermittent technology. Wind farms are becoming an increasingly offshore and onshore site [6-7].

Received: February 8, 2010. Accepted: July 7, 2010

The generated energy from wind energy can resolve natural gas or water into hydrogen and oxygen using AE. The generated hydrogen can then be compressed, stored and transported to the FC through pipelines. FC may utilize traditional fossil fuel such as coal, petroleum, natural gas or recycled energy with hydrogen and molecule such as marsh gas, methyl gas etc., but the power generation style of the FC is quite different from traditional power plants. High efficiency, low pollution, onsite installation, reusability of exhaust heat and wastes are some added advantages of this scheme [8-10]. Diesel generator serves the purpose of stand by unit. Both functions of storage and release of energy at the real time are the added inherent features of energy storage devices. Flywheel energy storage system (FESS) stores energy in the form of kinetic energy and may supply the same for the odd hour requirements while integrating the same with the renewable energy. The characteristic features of this device may be noted from the view points of high stored energy density, high power exchanging capability with the system, high conversion efficiency (80-90%) and increased pollution free operation. On the other hand, battery energy storage system (BESS) also stores energy in the form of kinetic energy. It may also play an important role in the power exchange program. As an economic utility application, BESS has been used as a potential source of energy storage devices [11]. Thus, WTG, AE, FC, DEG, FESS, and BESS may be a range of DGs.

Nuclear power plants, owing to their high efficiency, are kept at base load. On the other hand, generation from gas plants is very small and is suitable for varying load conditions. Both the units have no participation in automatic generation control (AGC) of a large power generation. Thus, AGC is mainly focused on thermal or hydro units for conventional power generation scheme [12-13].

Nanda *et al.* [12] has considered an interconnected hydro-thermal system in the continuous discrete mode using conventional integral (I) controller or proportional integral (PI) controller and it has been established in this work that maximum deviation and settling time are same for both the controllers. Thus, it is quite relevant that integral controller may be considered for the AGC loop.

Reheating in reheat turbines may be carried out in single or double stage. For all practical purposes, Nanda *et al.* [12] in the context of hydro-thermal AGC have established that a single stage reheat turbine may replace a double stage one. This has also been found to be true by Mukherjee and Ghoshal [13] in the context of automatic voltage regulator (AVR) and power system stabilizer (PSS) equipped AGC assisted thermal unit. Thus, it would be an appropriate approach to take single-stage reheat turbine for thermal unit.

A lot of literature exists for the tuning of single input conventional power system stabilizer (CPSS) parameters in the AVR loop of the generator. What about the interactive performance of dual input PSS [14] tuned AVR loop and integral controlled AGC loop with thermal unit for conventional power plant? Thus, it is quite pertinent to explore the interactive transient performance of AVR along with dual input PSS loop combined with thermal AGC loop. Particle swarm optimization (PSO) [15] is a population-based evolutionary algorithm. Survival of the fittest is the underlying concept of genetic algorithm (GA). On the other hand, simulation of the social behavior motivates the concept of PSO. In PSO, each candidate solution is associated with a velocity. Particles or the candidate solutions then *fly* through the search space. The velocity is constantly adjusted with the corresponding particle's and its companions' experience. Resultantly, particles move towards better solution areas. PSO is passing through various modifications and experiments with an attempt to enhance its searching ability and to converge faster with lesser time of execution [16-18].

Wavelet [19] is a tool to model seismic signals by controlling dilations and translations of a simple oscillatory function (the mother wavelet) of finite duration. The wavelet function possesses two properties viz. (a) the function integrates to zero, and (b) it is square integrable (meaning it has finite energy). Owing to these properties of the wavelet, as derived from the literature, it may be expected that both convergence and solution stability would be improved. It is possible to exploit this property of Wavelet theory and apply the same in PSO to overcome the premature convergence?

Kumar *et al.* in [20] have proposed an AGC control scheme pertaining to DG. This scheme has been interconnected with the power system. Analysis in the context of AVR and PSS equipped AGC model for thermal unit, was beyond the scope of this paper. Further, tunable parameters of few controllers were set by trial and error basis, and accordingly the performances were analyzed. Better quality responses may highly be demanded with optimally tuned parameters derived from applying any suitable optimization technique. Moreover, a more realistic power system model would have been taken into account and analyzed. The present work emphasizes on these issues.

Mallesham *et al.* in [21] have investigated the load frequency control of DG consisting of WTG, solar and DEG. The frequency bias calculation is very important in the power system dynamics and plays the key role in controller gains. This factor directly affects the individual components like diesel generators and, finally, overall performance of the DGs. So the selection of frequency bias is very crucial and has been addressed in [21]. In this work, energy storage devices are not considered. The frequency response analysis in the context of combined conventional power generation scheme and DG is beyond the scope of [21]. Basically, ref. [21] motivates the authors of the present work to consider a more realistic DG scheme.

The viability of superconducting magnetic energy storage (SMES) for power system dynamic performance improvement has been widely and vividly reported in the literature [22, 23]. Its application in real power system has invited problems from the view points of operation, maintenance and cost involvement. However, capacitive energy storage (CES) [13, 24] may be a better alternative choice to damp out the power frequency oscillation, following any perturbation in the power system. A CES is, practically, maintenance free. Unlike magnetic energy storage units, CES does not impose any environmental problem. The operation is quite simple and less expensive compared to SMES. SMES requires a continuously operating liquid helium system. In magnetic storage systems, continuous flow of current is required but CES does not demand so. Thus, as a corrective measure against power system perturbation, CES plays an important role to damp out local mode power system oscillations. In the context of AGC coordinated PSS equipped AVR model along with DG, it is quite relevant to investigate the further improvement in the transient performance by the application of CES. This concept is yet to be addressed in the state of the art literature.

Integration of GA's mutation operation into the PSO [15], proposed by Esmin *et al.* in [25], though alleviates the premature convergence (stagnation) of the particles, but mutating space is kept unchanged all the time throughout the search. It also keeps the mutating space fixed. Is it possible to have further improvement using varying mutation space?

2. Proposed Hybrid Model

A single machine infinite bus (SMIB) system [26], as shown in Figure 1, is considered. The hybrid DG is connected in the LT bus as shown in Figure 1. The MATLAB-SIMULINK representation of SMIB system with AVR, high gain thyristor exciter, synchronous generator, PSS loop, AGC loop and CES loop is shown in Figure 2.

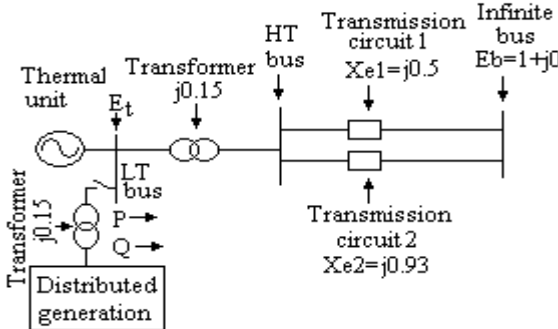


Figure 1. Single machine infinite bus system with distributed generation.

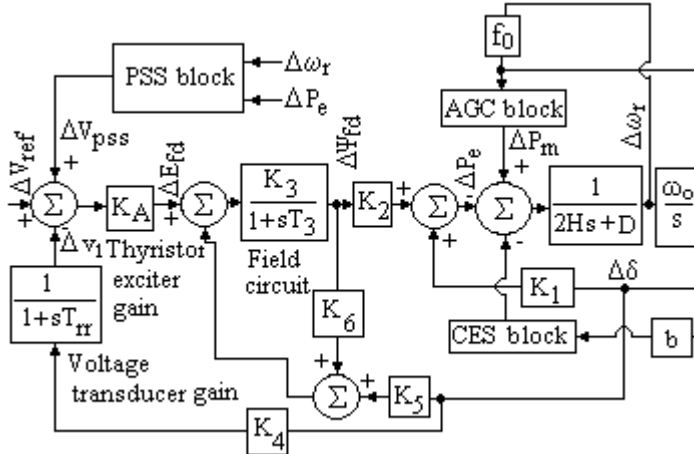


Figure 2. SMIB system with AVR, thyristor high gain exciter, synchronous generator, PSS block, DG included AGC block, and CES block.

A. Distributed generation configuration

The configuration of the proposed hybrid distributed generation scheme is a combination of conventional and distributed power generation schemes (Figure 3).

$$\Delta P_m = \Delta P_{hyd} + \Delta P_{deg} + \Delta P_{wtg} + \Delta P_{fc} - \Delta P_{fess} - \Delta P_{bess} \quad (1)$$

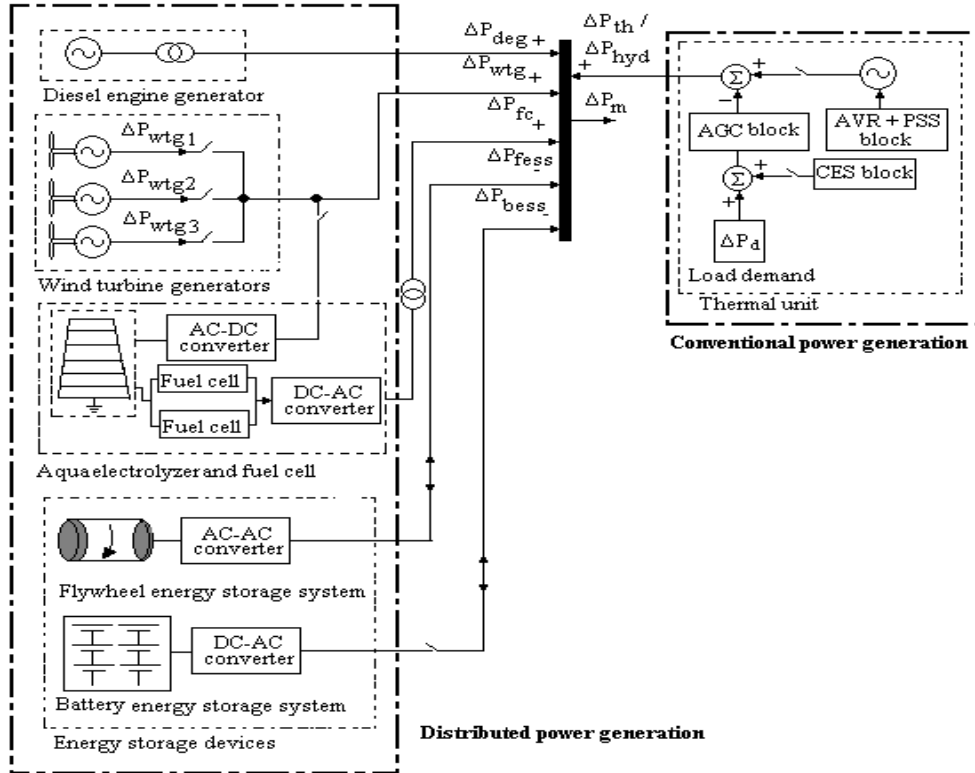


Figure 3. Block diagram of the studied hybrid power generation scheme with various DG schemes.

In the conventional power generation scheme, thermal power generation scheme with a single stage reheat turbine is considered. On the other hand, the DG comprise of WTG, AE, FC, DEG, FESS and BESS. The various components of the DG with transfer functions and parameter values are shown in [Table 1 \[20\]](#). The net incremental change in mechanical power (ΔP_m) is determined by the expression given in the following equation.

Table 1. Various components of DG with transfer functions and parameter values

Component	Transfer function	Notations		Parameter value
Aqua electrolyzer	$G_{ae}(s) = \frac{K_{ae}}{1 + s\tau_{ae}}$	$K_{ae} =$	gain of aqua electrolyzer	$K_{ae} = 1.0$
		$\tau_{ae} =$	time constant of aqua electrolyzer	$\tau_{ae} = 0.2 \text{ s}$
Battery energy storage system	$G_{fess}(s) = \frac{K_{bess}}{1 + s\tau_{bess}}$	$K_{bess} =$	gain of battery energy storage system	$K_{bess} = -1/300$
		$\tau_{bess} =$	time constant of battery energy storage system	$\tau_{bess} = 0.1 \text{ s}$
Diesel generator	$G_{deg}(s) = \frac{16.5 + 16.5s}{0.025s^2 + s}$	--	--	--
Flywheel energy storage system	$G_{fess}(s) = \frac{K_{fess}}{1 + s\tau_{fess}}$	$K_{fess} =$	gain of flywheel energy storage system	$K_{fess} = -1/100$
		$\tau_{fess} =$	time constant of flywheel energy storage system	$\tau_{fess} = 0.1 \text{ s}$
Fuel cell	$G_{fc}(s) = \frac{K_{fc}}{1 + s\tau_{fc}}$	$K_{fc} =$	gain of fuel cell	$K_{fc} = 1.0$
		$\tau_{fc} =$	time constant of fuel cell	$\tau_{fc} = 4.0 \text{ s}$
Wind turbine generator	$G_{wtg}(s) = \frac{K_{wtg}}{1 + s\tau_{wtg}}$	$K_{wtg} =$	gain of wind turbine generator	$K_{wtg} = 1.0$
		$\tau_{wtg} =$	time constant of wind turbine generator	$\tau_{wtg} = 1.5 \text{ s}$

B. Dual input conventional power system stabilizer configuration

The two inputs to dual-input PSS, unlike the conventional single-input ($\Delta\omega_r$) PSS, are $\Delta\omega_r$ and ΔP_e . In [14], the performance of IEEE type PSS3B is found to be the best one within the periphery of the studied system model. This dual input PSS configuration is considered for the present work and its block diagram representation is shown in Figure 4.

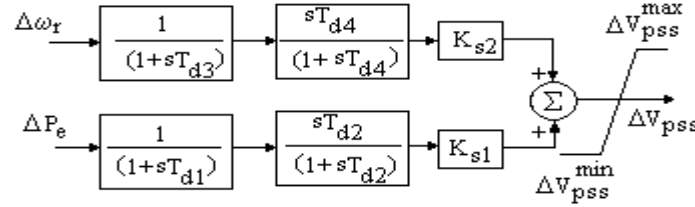


Figure 4. PSS (PSS3B) block subsystem of Figure 2.

C. Automatic generation control configuration

The main aim of AGC is zeroing of the area control error of each area of an interconnected multi-area generating stations so that the scheduled values of the system frequency and tie-line error is maintained. In general, two control variables associated with AGC scheme are deviations in system frequency and tie-line power exchange. These two variables give an idea about area controlled error (ACE) [16] and they are related as in the following equation.

$$ACE = (\Delta P_{tie} + b\Delta f) \quad (2)$$

In the present SMIB system, ACE is, basically, only $b\Delta f$.

D. Capacitive energy storage configuration

The basic configuration of a CES unit [13, 24] is shown in Figure 5. The storage capacitor is connected to the AC grid through a power conversion system (PCS) which includes an inverter/rectifier. Lumped capacitance C represents the discrete storage capacitors, the resistance R connected in parallel represents its dielectric and leakage losses. During normal operation of the grid, the capacitor can be charged to a set value of voltage (which is less than the full charge) from the utility grid. As the direction of current through the bridge converters cannot change, the main purpose of using the reversing switch arrangement with gate turn-off thyristors is to accommodate the change of direction of current in the capacitor during charging and discharging. During charging mode, switches S₁, S₄, are ON and switches S₂, S₃ are OFF. For discharging mode, S₂, S₃, are ON and S₁, S₄, are OFF.

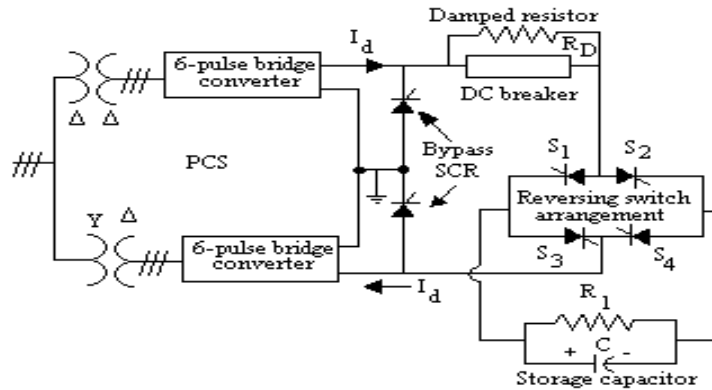


Figure 5. Configuration of capacitive energy storage.

3. Problem Formulation

A. Square error approach

The mathematical problem of the present work is to optimize the parameters of the PSS3B, the integral gain of the integral controllers installed in the AGC loop using any optimizing algorithm under parameter constraints. The parameters of the PSS3B are to be so tuned that some degree of relative stability and damping of electromechanical modes of oscillations are achieved. On the other hand, the objective of the controller design for the AGC loop also corresponds to the fulfillment of the same criteria. To satisfy all these requirements, square error (*SE*) objective function is adopted. The main focus here is minimization of *SE* with the help of any optimization technique, subject to the constraints of the parameters [14, 26].

B. Eigenvalue analysis

Another objective function chosen in the present problem is formulated as in equation (2). It is used for assessing the performance of *SE*-based optimization. It takes into account of two different eigenvalue-based objective functions reflecting damping factor, damping ratio of each of the electromechanical eigenvalues. The tuning of the system parameters corresponds to the minimization of the following equation.

$$\text{Minimize } J = J_1 + \alpha J_2 \quad (3)$$

Subject to $\forall i, \sigma_i > 0$, where σ_i is the real part of the i th eigenvalue of the system.

$J_1 = \sum_i (\sigma_0 - \sigma_i)^2$, if $\sigma_i \geq \sigma_0, \sigma_0 = -1.0$, σ_i is the real part of the i th eigenvalue. The relative stability is determined by σ_0 . $J_2 = \sum_i (\xi_0 - \xi_i)^2$, if (imaginary part of the i th eigenvalue) > 0.0 , ξ_i is the damping ratio of the i^{th} eigenvalue and $\xi_i < \xi_0$. Minimum damping ratio considered, $\xi_0 = 0.2$. Minimization of J_2 will minimize maximum overshoot by reduction in imaginary parts of the eigenvalues. The recommended value of α is 10.

4. Basic Wavelet Theory: A Concept

Certain seismic signals can be modeled by combining translations and dilations of an oscillatory function with a finite duration called a “wavelet”. Wavelet transform can be divided in two categories: continuous wavelet transform and discrete wavelet transform. The continuous wavelet transform $W(a,b)$ of function $f(x)$ with respect to a mother wavelet

$\psi(x) \in L^2(\mathfrak{R})$ is given by the following equation [19].

$$W_{a,b}(x) = \frac{1}{\sqrt{C_\psi}} \int_{-\infty}^{+\infty} f(x) \psi_{a,b}^*(x) dx \quad (4)$$

$$\text{where } \psi_{a,b}(x) = \frac{1}{\sqrt{a}} \psi\left(\frac{x-b}{a}\right), \quad x \in \mathfrak{R}, \quad a, b \in \mathfrak{R}, \quad a > 0 \quad (5)$$

In equation (3), $(*)$ denotes the complex conjugate, a is the dilation (scale) parameter, and b is the translation (shift) parameter. It is to be noted that a controls the spread of the wavelet and b determines its control position. A set of basis function $\psi_{a,b}(x)$ is derived from scaling and shifting the mother wavelet. The basis function of the transform is called the daughter wavelet. The mother wavelet has to satisfy the following admissibility condition.

$$C_\psi = 2\pi \int_{-\infty}^{+\infty} \frac{|\bar{\psi}(\omega)|^2}{\omega} d\omega < \infty \quad (6)$$

where $\bar{\psi}(\omega)$ the Fourier transform of $\psi(\omega)$ and is given by the following equation.

$$\bar{\psi}(\omega) = \frac{1}{\sqrt{2\pi}} \int_{-\infty}^{+\infty} \psi(x) \times e^{-j\omega x} dx \quad (7)$$

A function $f(x)$ having both smooth global variations and sharp local variations can be effectively represented by corresponding wavelet function $W(a, b)$. Inverse wavelet transform defined in equation (8) helps to recover the original function $f(x)$.

$$f(x) = \frac{1}{\sqrt{C_\psi}} \int_{-\infty}^{+\infty} \int_0^{+\infty} W(a, b) \frac{1}{\sqrt{a}} \psi\left(\frac{x-b}{a}\right) \frac{da \cdot db}{a^2} \quad (8)$$

A continuous function $\psi(x)$ is a ‘mother wavelet’ or ‘wavelet’ if it satisfies the following properties.

$$\text{Property I: } \int_{-\infty}^{+\infty} \psi(x) dx = 0 \quad (9)$$

Equation (9) demonstrates that the total positive momentum of $\psi(x)$ is equal to the total negative momentum of $\psi(x)$.

$$\text{Property II: } \int_{-\infty}^{+\infty} |\psi(x)|^2 dx < \infty \quad (10)$$

From equation (10), it may be inferred that most of the energy $\psi(x)$ is confined to a finite domain and is bounded.

5. Particle Swarm Optimization

PSO was first introduced by Kennedy and Eberhart [15] in 1995. Based on PSO concept, mathematical equations for the searching process are:

$$\text{Velocity updating equation: } v_i^{k+1} = v_i^k + c_1 \times r_1 \times (pBest_i - x_i^k) + c_2 \times r_2 \times (gBest - x_i^k) \quad (11)$$

$$\text{Position updating equation: } x_i^{k+1} = x_i^k + v_i^{k+1} \quad (12)$$

where c_1, c_2 are two positive constants representing cognitive and social learning rate, respectively, r_1, r_2 are two random numbers with uniform distribution in the interval of [0,1]. The steps of PSO are enumerated below.

Algorithm for PSO

Step 1	Initialize the swarm by assessing a random position in the problem hyperspace to each particle.
Step 2	Evaluate the fitness function for each particle.
Step 3	For each individual particle, compare the particle's fitness value with its $pBest$. If the current value is better than the $pBest$ value, then set this value as $pBest$ and the current particle's position x_i , as $pBest_i$.
Step 4	Identify the particle that has the best fitness. The value of its fitness function is identified as $gBest$ and its position as $gBest$.
Step 5	Update the velocities and positions of all the particles using Eqs. (11) and (12).
Step 6	Repeat steps 2-5 until a stopping criterion is visited (e.g., maximum number of iterations or a sufficiently good fitness value).

A. Particle swarm optimization with constriction factor approach and inertia weight approach

Empirical studies performed on PSO indicate that even when the maximum velocity and acceleration constants are correctly defined, the particles may still diverge, i.e., go to infinity; a phenomena known as “explosion” of the swarm. Two methods are proposed in the literature in order to control this “explosion”: *constriction factor approach* and *inertia constant approach*. Clerc and Kennedy [27] developed a method to control this “explosion”. The velocity of constriction factor approach can be expressed as follows:

$$v_i^{k+1} = CF \times \left(\omega \times v_i^k + c_1 \times r_1 \times (pBest_i - x_i^k) + c_2 \times r_2 \times (gBest - x_i^k) \right) \quad (13)$$

where

$$CF = \frac{2}{\left| 2 - \varphi - \sqrt{\varphi^2 - 4\varphi} \right|}, \quad c_1 + c_2 = \varphi > 4 \quad (14)$$

This PSO, in the present work, is termed as hybrid particle swarm optimization (HPSO).

B. Hybrid particle swarm optimization with mutation

To alleviate the problem of stagnation, Esmin *et al.* [25] incorporated the mutation operation of genetic algorithm (GA) into PSO. The mutation operation starts with a randomly chosen particle in the swarm and moves to different positions inside the search hyperspace by using mutation. The mutation operation safe guards PSO on landing into *stagnation*.

Algorithm for mutation in PSO

Step a:	Select a randomly element of the particle from the swarm.
Step b:	Generate ω randomly in the range $[0.0, 0.1 \times (para_{max}^j - para_{min}^j)]$, representing one-tenth of the length of the search space, where $para_{max}^j$, $para_{min}^j$ are the maximum and minimum value of the j^{th} particle, respectively.
Step c:	Generate r randomly in the range $[-1.0, +1.0]$.
Step d:	Perform: $\begin{cases} mut(x_j) = x_j - w, & r < 0 \\ mut(x_j) = x_j + w, & r \geq 0 \end{cases}$

This process may be modeled as given below. Steps a-d may be incorporated in the algorithm of PSO in between Step 4 and Step 5 to have hybrid particle swarm optimization with mutation (HPSOM) of the present work.

C. Hybrid particle swarm optimization with wavelet mutation (HPSOWM)

The mutation process postulates that the mutating search hyperspace is limited by ω and it may not be the best approach in fixing the size of the mutating space all the time along the search. It is proposed that every particle of the swarm will have a chance to mutate, governed by a user defined probability $p_m \in [0, 1]$. For each element, a random number between 0 and 1 will be generated such that if it is less than or equal to p_m , the mutation will take place on that element. Among the population, a randomly selected p^{th} particle and j^{th} element (within the boundary $[para_{\min}^j, para_{\max}^j]$) at iteration count t will undergo mutation as given in the following equation.

$$\bar{x}_j^p(t) = \begin{cases} x_j^p(t) + \sigma \times (para_{\max}^j - x_j^p(t)), & \text{if } \sigma > 0 \\ x_j^p(t) + \sigma \times (x_j^p(t) - para_{\min}^j), & \text{if } \sigma \leq 0 \end{cases} \quad (16)$$

$$\text{where } \sigma = \psi_{a, 0}(\phi) = \frac{1}{\sqrt{a}} \psi\left(\frac{\phi}{a}\right)$$

A Morlet wavelet (mother wavelet) defined in the following equation may be shown as in [Figure 6](#).

$$\psi(x) = e^{\frac{-x^2}{2}} \cos(5x) \quad (17)$$

$$\text{Thus, we have, } \sigma = \frac{1}{\sqrt{a}} e^{\frac{-(\phi)^2}{2}} \cos\left(5\left(\frac{\phi}{a}\right)\right) \quad (18)$$

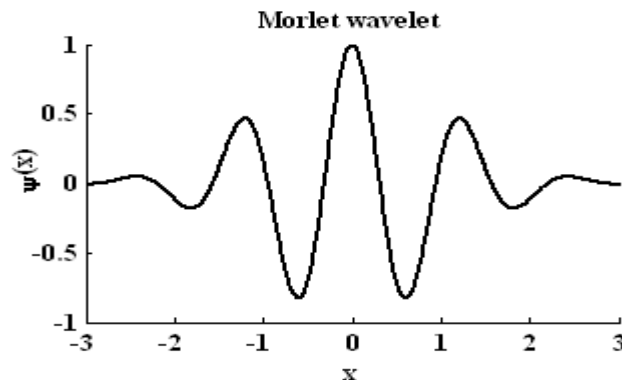
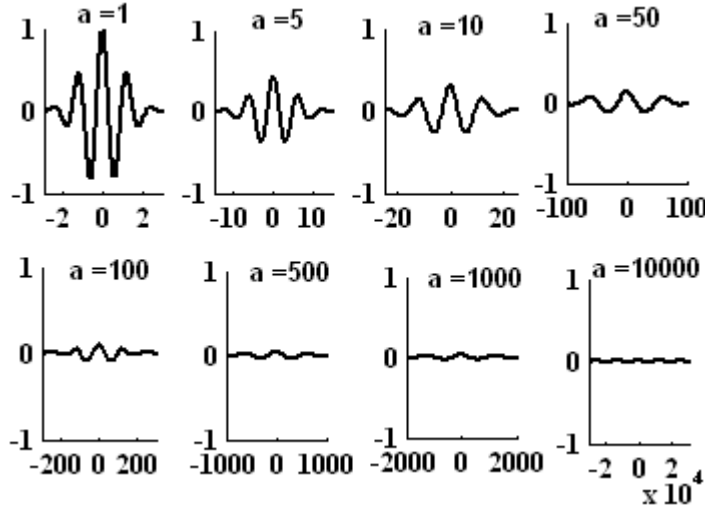


Figure 6. Morlet wavelet.

Figure 7. Dilated Morlet wavelet (x-axis: x, y-axis: $\psi_{a,0}(x)$).

Different dilated Morlet wavelets are shown in Figure 7. From this figure it is clear that as the dilation parameter a increases, the amplitude of $\psi_{a,0}(x)$ will be scaled down. In order to enhance the searching performance, this property will be utilized in mutation operation.

As over 99% of the total energy of the mother wavelet function is contained in the interval [-2.5, 2.5] (Property II), ϕ can be randomly generated from $[-2.5 \times a, 2.5 \times a]$. The value of the dilation parameter a is set to vary with the value of k/K in order to meet the fine-tuning purpose, where, k is the current iteration number and K is the total number of iterations. In order to perform a local search when k is large, the value of a should increase as k/K increases to reduce the significance of the mutation. Hence, a monotonic increasing function governing a and k/K may be written as given in the following equation.

$$a = e^{-\ln(g) \times (1 - \frac{k}{K}) \xi_{\omega m} + \ln(g)} \quad (19)$$

where $\xi_{\omega m}$ is the shape parameter of the monotonic increasing function, and g is the upper limit of the parameter a . After the operation of Wavelet mutation (WM), a new swarm is generated. This new swarm will repeat the same process. Such an iterative process will be terminated if a predefined number of iterations have been met.

A perfect balance between the exploration of new regions and the exploitation of the already sampled regions in the search space is expected in HPSOWM. This balance, which critically affects the performance of the HPSOWM, is governed by the right choices of the control parameters, e.g. swarm size (n_p), the probability of mutation (p_m), and the shape parameter of WM ($\xi_{\omega m}$). Changing the parameter $\xi_{\omega m}$ will change the characteristics of the monotonic increasing function of WM. The dilation parameter a will take a value to perform fine tuning faster as $\xi_{\omega m}$ is increasing. When $\xi_{\omega m}$ becomes larger, the decreasing speed of step size (σ) of the mutation becomes faster. In general, if the optimization problem is smooth and symmetric, it is easier to find the solution, and the fine tuning can be done in early iteration. Thus, a larger value of $\xi_{\omega m}$ can be used to increase the step size of the early mutation.

D. Craziness-based particle swarm optimization

The velocity updating strategy and inclusion of craziness, as proposed by Mukherjee and Ghoshal in [13], help to enhance the global search ability of PSO algorithm and the same is termed as craziness-based particle swarm optimization (CRPSO) in [13].

E. Craziness-based particle swarm optimization with mutation

Inclusion of mutation, as shown in the algorithm of mutation, in CRPSO [13] gives craziness-based particle swarm optimization with mutation (CRPSOM).

F. Craziness-based particle swarm optimization with wavelet mutation

Inclusion of wavelet mutation (discussed in section C) in CRPSO (discussed in section D) gives craziness-based particle swarm optimization with wavelet mutation (CRPSOWM) in the present work.

6. Input Data and Parameters

The best chosen maximum population size = 50, maximum allowed iteration cycles = 100, best p_{craz} = 0.2 (chosen after several experiments), $CF = 0.729$, best values of c_1 and c_2 are $c_1 = c_2 = 2.05$. The value of $v_i^{craziness}$ lies between 0.1 and 0.4. The SMIB parameters are in [14, 26]. Other model parameters are also given in Appendix. For simulation, 0.01 p.u. step load perturbation is applied either in reference voltage or in load. The other values are $\xi_{wm} = 2.0$, $g = 10000$, $p_m = 0.1$. The simulation implemented in MATLAB 7.1 software on a PC with PIV3.0G CPU and 512M RAM.

7. Simulation Results and Discussions

GA is taken for the sake of comparison. The major observations of the present work are as documented:

A. Sensitivity of the shape parameter ($\xi_{\omega m}$) for the WM

Table 2. Values of J and $SE (\times 10^6)$ under different values of the shape parameter ($\xi_{\omega m}$) of WM for thermal unit and thermal unit under different input perturbations

HPSOWM (0.01p.u. step perturbation in reference voltage)									
$\xi_{\omega m} = 0.2$		$\xi_{\omega m} = 0.5$		$\xi_{\omega m} = 1.0$		$\xi_{\omega m} = 2.0$		$\xi_{\omega m} = 5.0$	
J	SE	J	SE	J	SE	J	SE	J	SE
5.6011	4.6011	3.6011	3.6011	2.6017	2.6017	1.6011	1.6011	2.6066	1.9866
HPSOWM (0.01 p.u. step perturbation in load torque)									
$\xi_{\omega m} = 0.2$		$\xi_{\omega m} = 0.5$		$\xi_{\omega m} = 1.0$		$\xi_{\omega m} = 2.0$		$\xi_{\omega m} = 5.0$	
J	SE	J	SE	J	SE	J	SE	J	SE
4.5607	4.5607	3.5612	3.5612	2.5603	2.5603	1.5597	1.5597	2.5612	1.9712
CRPSOWM (0.01p.u. step perturbation in reference voltage)									
$\xi_{\omega m} = 0.2$		$\xi_{\omega m} = 0.5$		$\xi_{\omega m} = 1.0$		$\xi_{\omega m} = 2.0$		$\xi_{\omega m} = 5.0$	
J	SE	J	SE	J	SE	J	SE	J	SE
4.2831	4.1373	3.6751	3.3806	3.0023	2.3805	1.1134	0.9803	2.9492	1.6711
CRPSOWM (0.01 p.u. step perturbation in load torque)									
$\xi_{\omega m} = 0.2$		$\xi_{\omega m} = 0.5$		$\xi_{\omega m} = 1.0$		$\xi_{\omega m} = 2.0$		$\xi_{\omega m} = 5.0$	
J	SE	J	SE	J	SE	J	SE	J	SE
4.6397	4.1163	3.6478	3.6164	2.6274	2.6161	1.1636	0.9167	2.6609	0.6124

The values of J and SE offered by HPSOWM and CRPSOWM for the proposed hybrid model are presented in [Table 2](#). The values are with the inclusion of CES unit in the AGC block for the input operating condition being $P = 1.0$, $Q = 0.4$, $X_e = 0.4752$, and $E_t = 1.0$ (all are in p.u.). While performing this analysis, the value of g is fixed at 10000 and that of p_m is fixed at 0.1. It is to be noted here that if the optimization problem needs a more significant mutation to reach the optimal point, a smaller ξ_{wm} should be used and, conversely, if the algorithm needs to perform the fine-tuning faster, a larger ξ_{wm} should be used. It may be recommended that no formal method is available to choose the value of the parameter, ξ_{wm} , it is problem dependent. From the results presented in [Table 2](#) it is noticed that for this specific problem, the judicious choice of ξ_{wm} would be 2.0 as this value of ξ_{wm} offers the best result (bold faced in the table).

B. Sensitivity of the probability of mutation (p_m) for the WM

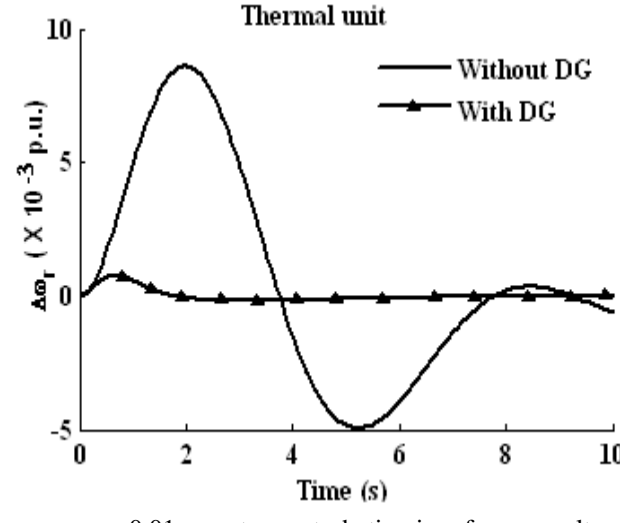
[Table 3](#) presents the values of J and SE for the proposed hybrid model for different values of p_m with $\xi_{wm} = 2.0$, and $g = 10000$. With lesser value of p_m like 0.01 or 0.05, the numbers of particles undergoing mutation are very less and the process may likely be trapped into local optima. On the other hand, with higher value of p_m like 0.2 or 0.5, a large number of particles undergo the mutation process and heavy fluctuation in the convergence rate of the objective function is noticed. Thus, moderate rate of mutation like $p_m = 0.1$ would be recommended (as evident from [Table 3](#) with least values of J as well as that of SE). Once again, it may be problem dependent. The results of interest are bold faced in this table.

Table 3. Values of J and SE ($\times 10^6$) under different values of the mutation probability (p_m) of WM under different input perturbations

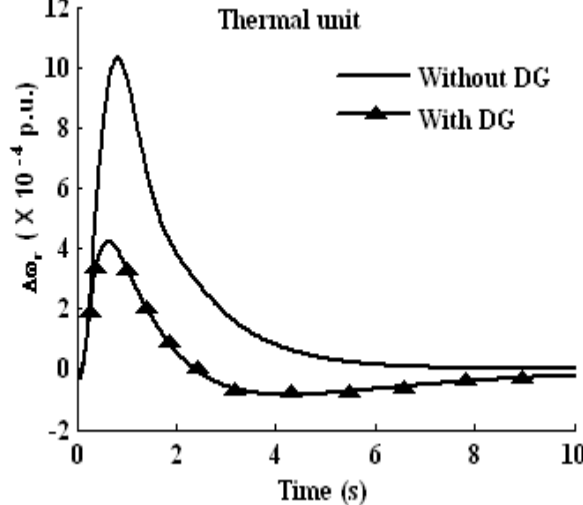
HPSOWM (0.01p.u. step perturbation in reference voltage)									
$p_m = 0.01$		$p_m = 0.05$		$p_m = 0.1$		$p_m = 0.2$		$p_m = 0.5$	
J	SE	J	SE	J	SE	J	SE	J	SE
5.6011	3.6011	2.6015	2.6015	1.8011	1.6011	2.7091	3.7091	3.6017	2.6017
HPSOWM (0.01 p.u. step perturbation in load torque)									
$p_m = 0.01$		$p_m = 0.05$		$p_m = 0.1$		$p_m = 0.2$		$p_m = 0.5$	
J	SE	J	SE	J	SE	J	SE	J	SE
5.5598	3.5598	2.5606	2.1606	1.8597	1.5597	2.5609	0.5609	3.5620	2.5620
CRPSOWM (0.01p.u. step perturbation in reference voltage)									
$p_m = 0.01$		$p_m = 0.05$		$p_m = 0.1$		$p_m = 0.2$		$p_m = 0.5$	
J	SE	J	SE	J	SE	J	SE	J	SE
5.6051	3.0010	2.1490	2.0826	1.4939	1.3808	2.7855	2.3818	3.9677	2.4409
CRPSOWM (0.01 p.u. step perturbation in load torque)									
$p_m = 0.01$		$p_m = 0.05$		$p_m = 0.1$		$p_m = 0.2$		$p_m = 0.5$	
J	SE	J	SE	J	SE	J	SE	J	SE
5.6479	3.0054	2.6430	2.0063	1.5064	1.4128	2.9414	2.6170	2.0492	2.0165

C. Performance evaluation of grid connected thermal unit using distributed generation

A comparison of the system transient performances of the grid connected thermal power system and the same equipped with DG is portrayed in [Figure 8](#) (operating conditions being $P=0.2$, $Q=-0.2$, $X_e=1.08$, $E_t=1.1$; all are in p.u.). [Figure 8\(a\)](#) is for 0.01 p.u. step change in reference voltage and [Figure 8\(b\)](#) is for 0.01 p.u. step change in load torque. From these subplots, it is prominent that the AGC is helping in the process of transient performance stabilization. Thus, improved transient performance is noticed with the usage of DG in a grid connected thermal unit with optimized system parameters.



(a) 0.01 p.u. step perturbation in reference voltage



(b) 0.01 p.u. step perturbation in load

Figure 8. Comparison of transient responses of the proposed hybrid models (without DG and with DG).

D. Performance evaluation of grid connected thermal unit using distributed generation and CES

Figures 9-10 depict the optimal transient performance of the power system corresponding to an operating condition of $P = 1.0$, $Q = 0.5$, $X_e = 0.4752$, $E_t = 1.0$ (all are in p.u.). From these figures it is noticed that due to the action of CES, the system transient performance is considerably improved. From these figures it is also noticed that the optimization performance of CRPSOWM-based optimization technique is the best one among the optimizations techniques handled by offering true optimal performance. The main task of CES may be attributed from the action of a sudden rise in the demand of load. Under this contingency condition, the stored energy in CES is almost immediately released through the PCS to the grid as line quality AC. As the governor and other control mechanisms start working to set the power system to the new equilibrium condition, the capacitor charges to its initial value of voltage. Similar is the action during sudden release of loads. The capacitor is immediately charged towards its full value, thus, absorbing some portion of the excess energy in the system, and as the system returns to its steady state, the excess energy absorbed is released and the capacitor voltage attains its normal value. Thus, improved transient performance is gained with the application of CES for the proposed hybrid system model.

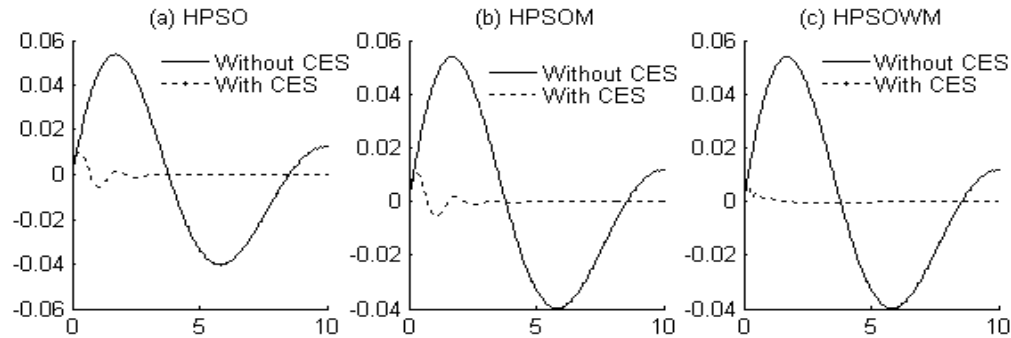


Figure 9. Different PSO-based system performance studies for DG assisted thermal unit without CES and with CES under 0.01 p.u. step perturbation in reference voltage (x-axis: Time (s); y-axis: $\Delta\omega_r \times 10^{-4}$ p.u.): (a) HPSO, (b) HPSOM, (c) HPSOWM.

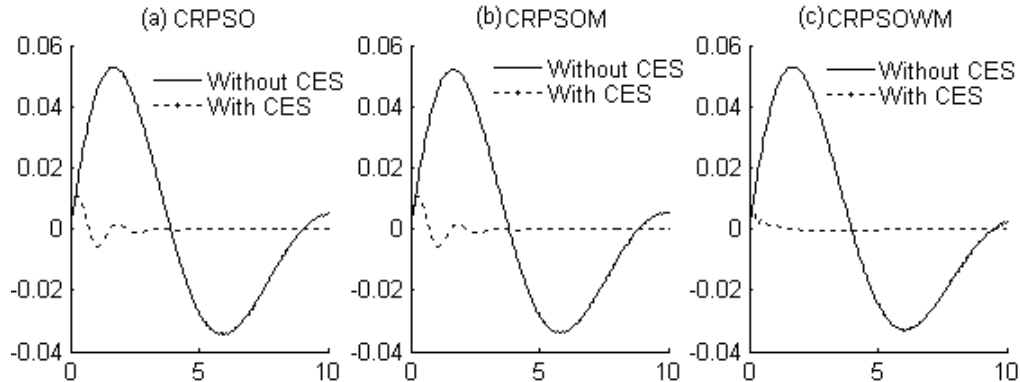


Figure 10. Different PSO-based system performance studies for DG assisted thermal unit without CES and with CES under 0.01 p.u. step perturbation in reference voltage (x-axis: Time (s); y-axis: $\Delta\omega_r \times 10^{-4}$ p.u.): (a) CRPSO, (b) CRPSOM, (c) CRPSOWM.

E. Convergence profile

The minimum values of J against number of iteration cycles of the swarm are recorded to get the convergence profiles for the algorithms. Figure 11(a) portrays the convergence profiles of minimum J for HPSO, HPSOM, and HPSOWM against 1% step perturbation in reference. The same for CRPSO, CRPSOM, and CRPSOWM are depicted in Figure 11 (b). From Figure 11(a), it is clear that HPSOWM converges faster than either HPSO or HPSOM. The same inference may be drawn with regard to convergence profile of CRPSOWM as compared to either CRPSO or CRPSOM. It is also noticed from Figure 11 that CRPSOWM is yielding the grand minimal value of J for the proposed system model with faster rate of convergence.

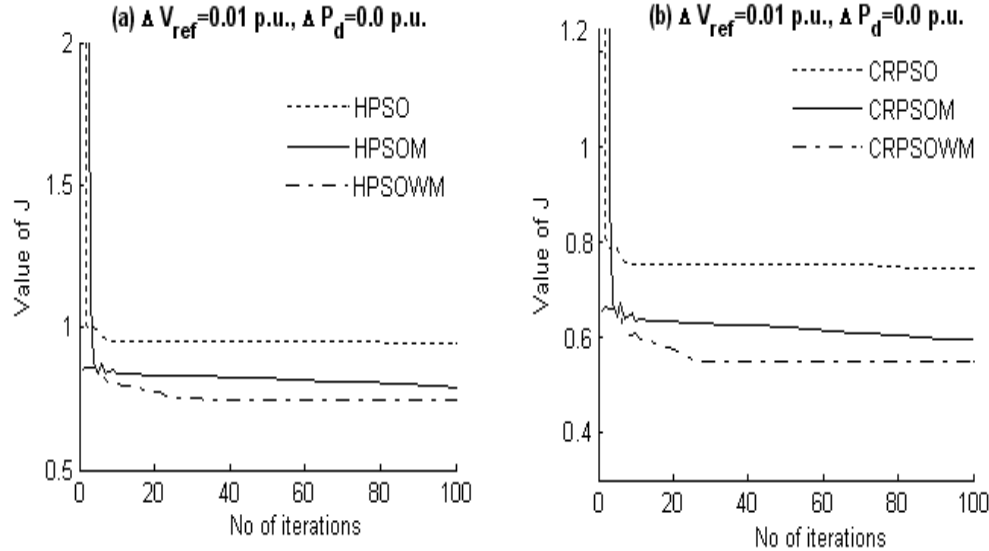


Figure 11. Comparison of convergence profiles of J values among different PSO techniques for thermal unit.

F. Statistical analysis of the results

The t -test is a statistical measure to evaluate the significant difference between two algorithms. The t -value will be positive if the first algorithm is better than the second, and it is negative if it is poorer. The t -value is defined as given in the following equation.

$$t = \frac{\bar{\alpha}_2 - \bar{\alpha}_1}{\sqrt{\left(\frac{\sigma_2^2}{\beta+1}\right) + \left(\frac{\sigma_1^2}{\beta+1}\right)}} \quad (20)$$

where $\bar{\alpha}_1$ and $\bar{\alpha}_2$ are the mean values of the first and second methods respectively; σ_1 and σ_2 are the standard deviations of the first and second methods respectively; and ξ is the value of the degree of freedom.

When the t -value is higher than 1.645 ($\beta = 49$), there is a significant difference between the two algorithms with a 95% confidence level. A statistical comparison of J and SE values among different algorithms after 50 trials is presented in Table 4. The t -test is a statistical measure to evaluate the significant difference between two algorithms. When the t -value is higher than 1.645 ($\beta = 49$), there is a significant difference between the two algorithms with a 95% confidence level.

The t-values between the CRPSOWM and the other optimization methods are presented in [Table 4](#). The t-value of all approaches is larger than 2.15 (degree of freedom = 49), meaning that there is a significant difference between the CRPSOWM and other methods with a 98% confidence level. GA-based results yield sub optimal results. Thus, from statistical analysis, it is clear that CRPSOWM-based optimization technique offers robust and promising results.

G. System transient response under simulation of fault

A fault of duration 220 ms at the LT sending end bus has been simulated at the instant of 2.0 s and the corresponding comparative transient response profiles of $\Delta\omega_r$ is displayed in [Figure 12](#). This figure shows that after the creation of the fault, the CES equipped system along with DG recovers from this abnormal situation with much lesser fluctuation in angular speed as compared to without CES but with DG system model. Thus, inclusion of CES in the DG assisted power system exhibits superb dynamic response having lesser amplitude of angular speed deviation (both undershoot and overshoot) and lesser settling time under fault and subsequent clearing condition.

Table 4. Comparison among different optimization algorithms (Input operating conditions: $P = 1.0$, $Q = 0.4$, $X_e = 1.08$, $E_t = 1.0$, all are in p.u.), (Rank 1: Best, Rank 7: Worst)

Type of perturbations	Parameter	GA	HPSO	HPSOM	HPSOWM	CRPSO	CRPSOM	CRPSOWM
0.01 p.u. step perturbation in reference voltage	J	2.9456	1.6822	1.6219	1.6011	0.9176	0.6253	0.6107
	$SE (\times 10^6)$	2.7523	2.6022	1.8019	1.5011	0.8176	0.6153	0.6007
	Run time (s)	967.87	931.75	932.42	932.70	958.18	959.42	959.81
	Min	2.5467	1.6021	1.5311	1.4022	1.2021	0.5729	0.5719
	Max	3.9810	3.6171	8.114	7.914	3.912	3.425	2.914
	Std. div.	1.1923	0.9972	0.9326	0.8873	0.8531	0.7373	0.3391
	Mean	1.9234	1.4323	1.1131	1.0781	0.9921	0.8807	0.6081
	t-test	7.5030	5.5332	3.5985	3.4987	2.9578	2.3752	NA
0.01 p.u. step perturbation in load torque	Rank	7	6	5	4	3	2	1
	J	2.1234	1.6019	1.6011	1.6022	0.6007	0.6176	0.6053
	$SE (\times 10^6)$	2.1123	1.6019	1.6011	1.6022	0.5729	0.5719	0.5723
	Run time (s)	968.23	931.750	932.422	932.703	958.188	959.422	959.812
	Min	2.8923	1.6579	1.6123	1.6112	1.6023	1.5719	0.5729
	Max	9.2452	3.617	8.114	7.914	9.1100	3.925	7.914
	Std. div.	1.1234	0.9172	0.7326	0.6373	0.5546	0.4001	0.3003
	Mean	1.7865	1.3922	1.2131	0.9877	0.7892	0.6995	0.5452
Over all ranking (average ranking number)	t-test	7.5481	6.2057	5.9649	4.4130	2.7357	2.1810	NA
	Rank	7	6	5	4	3	2	1

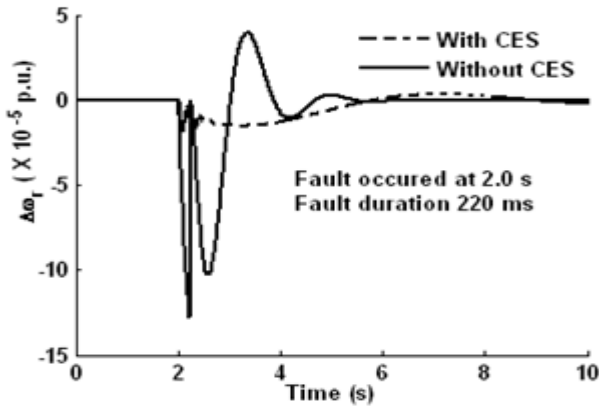


Figure 12. Comparison of transient responses of $\Delta\omega_r$ for DG assisted thermal unit without CES and with CES under different operating conditions and occurrence and subsequent removal of the fault at the LT bus.

Conclusion

A proper integration of DG units with traditional generating unit is carried out for the purpose of transient stability study. DG units like WTG, AE, FC, DEG, FESS and BESS are present. The traditional unit is considered as thermal unit with single stage reheat turbine. The thermal unit is equipped with AVR, dual input PSS like PSS3B, integral controlled AGC loop and CES loop. Integral-controlled AGC loop of such an integrated hybrid module is properly tuned. Parameters of the dual input PSS (IEEE PSS3B) are optimally tuned yielding optimal performance. DG is assisting in the transient stabilization process of the conventional thermal power system. With the inclusion of CES in the proposed DG assisted power system considerable improvement in the transient performance is noticed. With reference to the second and third authors' previous works in the field of PSO, earlier termed as CRPSO, the present work has proposed the incorporation of the Wavelet mutation concept in that CRPSO and termed as CRPSOWM. This newly entrant PSO technique in the PSO family explores the properties of Wavelet theory to explore the solution space more effectively on yielding the optimal solution and, thereby, offers better quality solution with faster convergence rate. Robustness of the proposed CRPSOWM technique over a range of PSO techniques and GA is noticed from statistical analysis of the results. Thus, application of capacitive energy storage unit may be successfully practically implemented for improving transient performance of such a DG assisted hybrid power system model.

References

- [1] J. W. M. Cheng, F. D. Galiana, D. T. McGillis, "Studies of bilateral contracts with respect to steady-state security in a deregulated environment," *IEEE Trans. Power Systems*, vol. 13, pp. 1020-1025, August 1998.
- [2] J. M. Arroyo, A. J. Conejo, "Multiperiod auction for a pool-based electricity market," *IEEE Trans. on Power Systems*, vol. 17, pp. 1225-1231, November 2002.
- [3] J. Hall, R. G. Colclaser, "Transient modeling and simulation of a tubular solid oxide fuel cell," *IEEE Trans. on Energy Conversion*, vol. 14, pp. 749-753, September 1995.
- [4] Y. H. Kim, S. S. Kim, "An electrical modeling and fuzzy logic control of a fuel cell generation system," *IEEE Trans. on Energy Conversion*, vol. 14, pp. 239-244, June 1999.
- [5] European Wind Energy Association. (2002). *Wind force 12*, [Online]. Available: <http://www.ewea.org/doc/WindForce12.pdf>.
- [6] P. Wang, R. Billinton, "Reliability benefit analysis of adding WTG to a distribution system," *IEEE Trans. on Energy Conversion*, vol. 16, pp. 134-139, June 2001.

- [7] N. Kodama, T. Matsuzaka, N. Inomata, "The power variation control of a wind generator by using probabilistic optimal control," *Trans. of Institute of Electrical Engineers Japan*, vol. 121-B, pp. 22–30, 2001.
- [8] Y. H. Li, S. S. Choi, S. Rajakaruna, "An analysis of the control and operation of a solid oxide fuel-cell power plant in an isolated system," *IEEE Trans. on Energy Conversion*, vol. 20, pp. 381–387, June 2005.
- [9] L. Gao, R. A. Dougal, S. Liu, "Power enhancement of an actively controlled battery/ultra capacitor hybrid," *IEEE Trans. on Power Electronics*, vol. 20, pp. 236–243, January 2005.
- [10] K. Ro, S. Rahman, "Two-loop controller for maximizing performance of a grid-connected photovoltaic-fuel cell hybrid power plant," *IEEE Trans. on Energy Conversion*, vol. 13, pp. 276–281, September 1998.
- [11] N. Hatziargyrio, M. Donnelly, M. Takasaki, *et al.* "Modeling new forms of generation and storage," *CIGRE TF.01.10, Fifth draft* 2000.
- [12] J. Nanda, A. Mangla, S. Suri, "Some new findings on automatic generation control of an interconnected hydrothermal system with conventional controllers," *IEEE Trans. on Energy Conversion*, vol. 21, pp. 187-194, March 2006.
- [13] V. Mukherjee, S. P. Ghoshal, "Application of capacitive energy storage for transient performance improvement of power system," *Electric Power Systems Research*, vol. 79, pp. 282-294, February 2009.
- [14] S. P. Ghoshal, A. Chatterjee, V. Mukherjee, "Bio-inspired fuzzy logic based tuning of power system stabilizer," *Expert System with Application*, vol. 36, pp. 9281-9292, July 2009.
- [15] J. Kennedy, R. C. Eberhart, "Particle swarm optimization," *Proc. IEEE International Conference on Neural Networks*, pp. 1942-1948, 1995.
- [16] S. P. Ghoshal, "Optimization of PID gains by particle swarm optimization in fuzzy based automatic generation control," *Electric Power Systems Research*, vol. 72, pp. 203-212, May 2004.
- [17] V. Mukherjee, S. P. Ghoshal, "Intelligent particle swarm optimized fuzzy PID controller for AVR system," *Electric Power Systems Research*, vol. 72, pp. 1689-1698, October 2007.
- [18] Y. D. Valle, G. K. Venayagamoorthy, S. Mohagheghi, J. C. Hernandez, E. G. Harley, "Particle swarm optimization: basic concepts, variants and applications in power systems," *IEEE Trans. on Evolutionary Computation*, vol. 12, pp. 171-194, April 2008.
- [19] N. M. Pindoriya, S. N. Singh, S. K. Singh, "An adaptive wavelet neural network-based energy price forecasting in electricity markets," *IEEE Trans. on Power Systems*, vol. 23, pp. 1423-1432, August 2008.
- [20] B. S. Kumar, S. Mishra, N. Senroy, "AGC for distributed generation," *Proc. International Conference on Sustainable Energy Technologies*, pp. 89 – 94, 2008.
- [21] Mallesham, S. Mishra, A. N. Jha, "Maiden application of Ziegler-Nichols method to AGC of distributed generation system," *Proc. Power System Conference and Exposition IEEE/PES*, pp. 1-7, 2009.
- [22] S. C. Tripathy, K. P. Juengst, "Sampled data automatic generation control with superconducting magnetic energy storage in power systems," *IEEE Trans. on Energy Conversion*, vol. 12, pp. 187-192, June 1997.
- [23] S. Banerjee, J. K. Chatterjee, S. C. Tripathy, "Application of magnetic energy storage unit as load frequency stabilizer," *IEEE Trans. on Energy Conversion*, vol. 5, pp. 46-51, March 1990.
- [24] S. C. Tripathy, R. Balasubramanian, P. S. Chandramohanan Nair, "Small rating capacitive energy storage for dynamic performance improvement of automatic generation control," *Proc. IEE-C*, vol. 138, pp. 103–111, January 1991.

- [25] A. Esmin Ahmed, G. Lambert-Torres, A. C. Zambroni de Souza, "A hybrid particle swarm optimization applied to loss power minimization," *IEEE Trans. on Power Systems*, vol. 20, pp. 859-866, May 2005.
- [26] P. Kundur, *Power System Stability and Control*, India: Tata-McGraw-Hill, 2006.
- [27] M. Clerc, J. Kennedy, "The particle swarm-explosion, stability, and convergence in multidimensional complex space," *IEEE Trans on Evolutionary Computation*, vol. 6, pp. 58-73, February 2002.



A. Chatterjee was born in 1974 at Nirsha, Dhanbad, Bihar (Presently, Jharkhand), India. He received his graduation in electronics and power engineering from Nagpur University, Nagpur, India and post-graduation in high voltage engineering from Jadavpur University, Jadavpur, West Bengal, India. Currently, he is with electrical engineering department of Asansol Engineering College, Asansol, West Bengal, India and is pursuing Ph.D. degree from National Institute of Technology, Durgapur, West Bengal, India. His research interest includes small signal stability, restructured power systems and evolutionary computing techniques. He will be available at nirsha_apurba@rediffmail.com.

Mr. Chatterjee is an associate member of The Institution of Engineers (India).



S. P. Ghoshal received B. Sc, B. Tech degrees in 1973 and 1977, respectively, from Calcutta University, India. He received M. Tech degree from IIT (Kharagpur) in 1979. He received Ph.D. degree from Jadavpur University in 1992. Presently, he is acting as professor of electrical engineering department of National Institute of Technology, Durgapur, West Bengal, India. His research interest is application of soft computing intelligence to various fields of power systems and antenna. He will be available at spghoshalnitdgp@gmail.com.

Prof. Ghoshal is member of IEEE and fellow of The Institution of Engineers (India).



V. Mukherjee was born in 1970 at Raina, Burdwan, West Bengal, India. He received his graduation in electrical engineering and post graduation in power system from B.E. College, Shibpur, Howrah, India and B.E. College (Deemed University), Shibpur, Howrah, India, respectively. He received his Ph.D. degree from National Institute of Technology, Durgapur, India. Presently, he is an assistant professor in the department of electrical engineering, Indian School of Mines, Dhanbad, Jharkhand, India. His research interest includes small signal stability analysis, distributed generation and evolutionary computing techniques. He will be available at vivek_agamani@yahoo.com.

Dr. Mukherjee is a member of The Institution of Engineers (India).